TITLE GOES HERE AND WILL BE AUTOMATICALLY SET IN ALL CAPS

Draft of April 12, 2021 at 14 : 43

BY

MIN-HSIU HSU

THESIS

Submitted in partial fulfillment of the requirements
for the degree of Master of Science in Mechanical Science and Engineering
in the Graduate College of the
University of Illinois at Urbana-Champaign, 2021

Urbana, Illinois

Adviser:

Assistant Professor Chenhui Shao

Abstract

Non-destructive evaluation (NDE) and fatigue damage assessment are crucial for quality control of remanufacturing processes. However, critical challenges exist in the development of NDE techniques for used components: individual NDE technology is only sensitive to specific fatigue conditions; analytics methods are lacking for quantitatively measuring accumulated mechanical damage and conducting prognostics in an early fatigue stage. In this paper, we propose a machine learning-based NDE technology by combining the strengths of linear ultrasonic (LU) and nonlinear ultrasonic (NLU) testings to detect defects at various length scales. Besides, a remaining useful life (RUL) estimation framework with hierarchical classifiers and S-N curves for identifying fatigue damage levels and inferring residual fatigue life of recycled parts is developed. In addition, regression models for estimating residual stress and full width at half maximum (FWHM) of x-ray diffraction (XRD) peak by ultrasonic testings are investigated. The effectiveness of the proposed methods are demonstrated using life cycle fatigue testing data for 5052-H32 aluminum alloy. This research aims to provide a screening system for end-of-life (EoL) products and lead to an increasing usage of secondary materials for remanufacturing and high-quality products.

To my parents, for their love and support.

Acknowledgments

Table of Contents

List of Tables

List of Figures

LIST OF ABBREVIATIONS

Chapter 1

Introduction

Remanufacturing has increasingly received attention because of its energy-saving, eco-friendly, and cost-efficient characteristics. Remanufactured products has been presented in automotive, aerospace, and industrial machinery industry. For example, in the automotive industry, Ford Motor has been recycled and remanufactured components such as engine, transmission, car body, etc., as a long-term tradition. In short, remanufacturing is a process of returning a used product to at least original performance specification from the customers' perspective. To achieve this, secondary materials screening for quality control in remanufacturing process by estimating the quantities of interest, e.g., remaining useful life (RUL) and residual stress in incoming recycled end-of-life (EoL) products, becomes an essential step and is crucial in increasing the usage of recycled materials.

In recycled components, material fatigue damage is universally presented and it is one of the most influential factors that determines the RUL of a used product. Material fatigue has resulted in many catastrophic accidents in the history and has been studied for many decades; however, the fatigue damage level is hard to be monitored in real world environments due to the stochastic nature of fatigue behaviors and undetermined loading conditions [1], which is a critical issue to be addressed.

To quantitatively study fatigue damage in materials, non-destructive evaluation (NDE) methods have been developed [2]. NDE, also known as non-destructive testing (NDT), is a technique to evaluate material properties without causing damage to the testing parts. For instance, linear ultrasonic (LU) and nonlinear ultrasonic (NLU) testings send ultrasonic waves which propagate in a material and analyze the response signals to evaluate material degradation. Although there exist a variety of NDE techniques, each of these methods is only sensitive to a few specific fatigue conditions and is limited to detecting defects in certain length scales. Figure 1.1 illustrates the

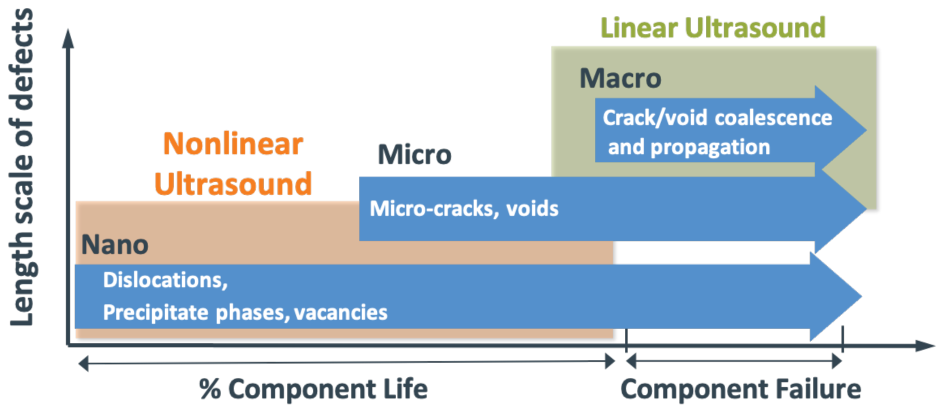

Figure 1.1: Capability of defect detection for LU and NLU testings

detectable length scales of LU and NLU testings, where LU testing is robust at detecting macro-scale defects. In contrast, NLU techniques measure nonlinear material parameters to detect defects which are orders of magnitude smaller than the probing wavelength (in e.g. stainless steels, typically on the order of 1mm), providing an important data source of early stage damage characterization.

There is a lack of research on the estimation and prognosis of RUL of EoL components in the remanufacturing industry even though, with state-of-the-art machine learning (ML) models, RUL estimation has been successfully applied in many industrial components, e.g., bearing [3, 4, 5], gear [6], turbofan engine [7, 8, 9], and lithium-ion battery [7, 10, 11]. Unlike the examples in the literature, the possible difficulties for RUL estimation in remanufacturing are: *a*) Continuous and in-situ measurements are not available, i.e., unable to know the historical measurements of a recycled component. *b*) Environmental noises can affect the performance of in-situ sensors as well as the built algorithms. *c*) The data in this field is hard to collect and thus is not adequate to build robust data-driven models.

In this research, we proposed a ML-based NDE methodology for the quantification and prognostics of accumulated fatigue damage in recycled materials. First, we integrate LU and NLU testings to leverage the strength of each individual sensor, which has the potential of estimating different fatigue conditions simultaneously. Second, with multi-output hierarchical classifiers, a RUL estimation framework is developed by predicting the loading condition as well as the percentage of fatigue life that a component has undergone, and then the RUL is estimated from a S-N curve. In the proposed approach, both ultrasonic testings sever as ex-situ measurement methods to predict the loading history of a recycled component. Therefore, without continuous monitoring data of a component from its healthy state, the RUL can be inferred by using the current measurement only. Besides, a residual stress measurement method based on the proposed NDE methodology and ML techniques is also investigated, which shows the potential of being an efficient method in terms of test speed and cost.

This research is targeted to metals that are widely used in a number of industry sectors. In this preliminary study, the target material is 5052-H32 aluminum alloy which is widely used in truck and auto industries. Life cycle fatigue testings were conducted in different settings to construct a comprehensive database for fatigue progression in the target material. The fatigued specimens were later examined by ultrasonic as well as X-ray diffraction (XRD) measurement. Here, XRD measurements serve as the calibration for residual stress and full width at half maximum (FWHM) estimation. After that, the proposed NDE methodology and prediction framework were developed and tested on the collection of fatigued samples.

The goal of this research is to not only enable effective materials screening but also provide valuable information for the process optimization and control of downstream remanufacturing processes. As such, an effective NDE method that is applicable on the factory floor will lead to greater material recycling and improved quality of products that are produced using recycled materials.

The remaining of this thesis is organized as follows. Chapter 2 provides the literature review of the related topics. Chapter 3 describes the experimental setup and procedures including the design of experiments, life cycle fatigue testing, ultrasonic and XRD measurements. Chapter 4 introduces the ML model development procedure used in both Chapter 5 and Chapter 6 where the proposed RUL estimation framework and residual stress measurement method are presented, respectively, with the case study on our fatigue test dataset. Finally, in Chapter 7, the contributions of this thesis are summarized and future research directions are mentioned.

Chapter 2

Literature Review

2.1 Fatigue damage assessment

Fatigue damage is a critical issue in engineering due to the concern of safety, and accurate estimation of fatigue damage has been a decades-long study in areas such as remanufacturing, transportation equipment, and structural health monitoring. Santecchia et al. provides an extensive overview of fatigue damage models for metals from various perspectives including linear damage rule, continuum damage mechanics, multi-axial as well as variable amplitude loading, energy-based methods, and stochastic-based approaches. However, none of these can be universally accepted because of the complexity of fatigue damage behaviors in reality [1].

2.2 NDE of fatigue damage

In many practical scenarios, non-destructive evaluation/testing has been adopted to quantify fatigue damage by investigating the correlation between measurement data and material deterioration [12]. Some common NDE techniques for evaluating fatigue damage are infrared thermography [13], holographic interferometry [14], microwave [15], ultrasonic testing, magnetic methods [16], acoustic emission approaches, and electrical resistance methods. While numerous NDE methods are available, each of these techniques has its own characteristics and thus is only sensitive to only one or a few specific applications. Recently, Wisner et al. presented a review of NDE in fatigue and suggested that when combined, NDE methods have been shown to improve the robustness of damage detection by complementing each other [2].

2.3 LU and NLU applications

Among various NDE techniques, LU and NLU has demonstrated its applicability in fatigue damage assessment [17, 18, 19, 20], defect classification [21, 22], and residual stress measurement [23, 24, 25] in materials. In terms of fatigue damage, Joshi and Green showed that ultrasonic attenuation is an indicator of fatigue damage in experiments performed on aluminum and steel [17]. Nagy introduced an experiment setup to monitor the second-order acoustic-elastic coefficient during the cyclic loading test, and demonstrated that the change in nonlinear parameter, which monotonically increases as a function of number of cycles applied, is substantially more than the corresponding change in linear parameters, wave velocity and attenuation [18]. Matlack et al. presented a comprehensive review of second harmonic generation (SGM) measurements for the NDE of fatigue, thermal aging, and radiation-induced damage [19]. An analytical model developed by Cantrell used a material nonlinearity parameter β extracted from SGM to quantify the level of dislocation substructures and cracks that evolve during cyclic fatigue of planar slip metals, which presented the potential of using SGM to assess the remaining life of the material. Nonetheless, practical implementation requires that the loading and environmental conditions of fatigue are given [20].

2.4 ML-aided NDE

In recent years, machine learning has been commonly applied to NDE techniques in the automated recognition of patterns in testing signals and the outcome of interest such as fatigue damage levels, defect types, and welding quality. For example, Baumgartl et al. implemented a CNN-based in-situ thermographic monitoring system to identify defects produced during the additive manufacturing process of H13 steel [26]. An optical interferometry-based real-time quality prediction system using ANN in laser beam welding was developed by Stadter et al. [27]. Loutas et al. proposed a framework utilizing AE signals for fatigue damage prognostics in composite materials with hidden semi Markov model and Bayesian neural network [28]. For ultrasonic testings, various features were engineered through fast Fourier transform, wavelet transform, and statistical methods, and fed into ML models for defect classification in [21, 22]. ML-aided NDE are fast growing and more applications such as RUL estimation and residual stress measurement exist in the literature.

2.5 RUL estimation

RUL estimation has received broad interests these days in many applications such as bearing [3, 4, 5], gear [6], turbofan [7, 8, 9], and lithium-ion battery [7, 10, 11]. However, there is relatively fewer recent RUL researches directly studying material fatigue. In early years, Ray and Tangirala presented a nonlinear stochastic model for predicting fatigue life in 2024-T3 aluminum alloy based on extended Kalman filter [29]. Peng et al. proposed a Bayesian updating framework based on a physics-based fatigue crack growth model with crack length estimated from piezoelectric sensor signals by a regressor to perform the lap joint fatigue life prognosis for 2024-T3 aluminum alloy [30]. Banerjee et al. recently utilized optical and acoustic NDE techniques accompanied with Kalman filter and particle filter to predict RUL in glass fiber reinforced polymer [31]. In the literature, most of the RUL research papers associated with fatigue damage rely on physical fatigue modeling and state-space models, e.g., particle filter method. Since physical models contain assumptions and approximation, physical models are limited in complex application scenarios.

Although lots of data-driven approaches for RUL estimation existed [32, 33] especially as deep learning has become increasingly prevalent these years [34], the successful cases generally require a sufficient amount of data for training the state-of-the-art models [4, 5, 8, 9, 11]. In the field of estimating residual fatigue life, Lim et al. developed a data-driven RUL prognosis technique with an artificial neural network (ANN) and nonlinear ultrasonic measurements for 6061-T6 aluminum [35]. There is, still, much fewer data-driven researches available for residual fatigue life estimation.

Moreover, we barely found methods that makes RUL estimation by taking only the measurement at current time step as input, which is the situation we envision for our application on the screening process in the remanufacturing industry. The existing examples using approaches such as Kalman filter

[29], particle filter [31], and recurrent neural network [9] make predictions based on successive measurements. To tackle the lack of previous observations, one relevant research is Mazhar et al.'s work on EoL products, where the authors integrated Weibull analysis and an ANN model taking a single measurement to assess the RUL of components for reuse. Due to the lack of data, nonetheless, synthetic data is needed for training the ANN in this work [36].

2.6 Residual stress measurement with ultrasounds

Residual stresses are often existed in mechanical components and have been recognized as a main factor of fatigue failure [37]. Residual stress measurement, therefore, has been an active area. A review of recent progress of residual stress measurement from GUO et al. provides a comparison between a variety of methods from the aspects of resolution, applicable object, and limitations [38]. Specifically for ultrasonic testing, the theory of acoustoelastic effect (the presence of stress in solids causes changes in the speeds of ultrasonic waves) for measurement of residual stress has been studied in [23]. Tanala et al. compared ultrasonic velocity measurements with X-ray diffraction in determining residual stress across a steel pipe and a alloy plate, which stated that ultrasonic techniques are more efficient in test volume and the cost of equipment [24]. In recent studies, Liu et al. implemented a testing system to analyze the accuracy and feasibility of residual stress measurement in 6063-T4 aluminum alloy by ultrasonic longitudinal critically refracted wave based on acoustoelastic theory [25].

Chapter 3

Experimental Dataset

This chapter describes the dataset and the experimental procedure used in this research for developing machine learning applications. First, the cyclic fatigue testing was conducted till the fracture of a specimen to acquire the fatigue characteristics of a material. Second, to mimic the scenarios in the remanufacturing industry, interrupted fatigue testing was utilized to produce specimens at different fatigue levels as a representation of end-of-life products. Then, linear and nonlinear ultrasound measurements are used to evaluate the fatigue damage of those specimens stopped at the predetermined number of cycles in the interrupted fatigue test. Besides, the residual stress and full width at half maximum data from X-ray diffraction are also presented.

3.1 Life cycle fatigue testing

The life cycle fatigue testing aims to collect fatigue life data to understand the fatigue behavior of our targeted material. The fatigue life of a material is defined as the total number of cycles that a material can sustain under a specified loading condition. In order to develop the S-N curve of a material, the material is tested at different loading stress amplitudes, and the fatigue test is repeated multiple times for each loading stress amplitude to account for the variance of fatigue life.

The fatigue testing in this research is led by Prof. Li's group at the Penn State University. The targeted material is 5052-H32 aluminum alloy which is widely used for car body construction in the automotive industry. Figure 3.1 shows the dimension of the specimen and the test machine. Three loading amplitudes, 11.7, 12.7, and 14.7 kN for the cyclic fatigue testing are selected to develop the S-N curve which is shown in Figure 3.2.

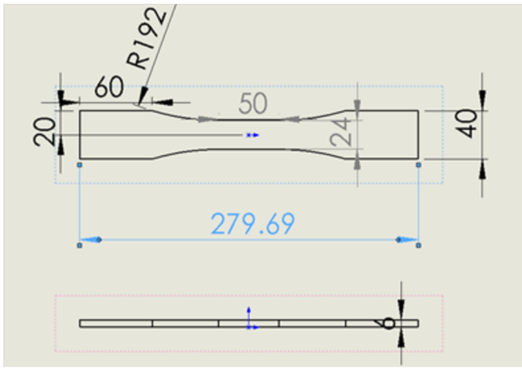

(a) Schematic of the 5052-H32 aluminum alloy specimen

(b) MTS 100KN Landmark fatigue testing system at Prof. Jingjing li's lab

Figure 3.1: Life cycle fatigue testing setup

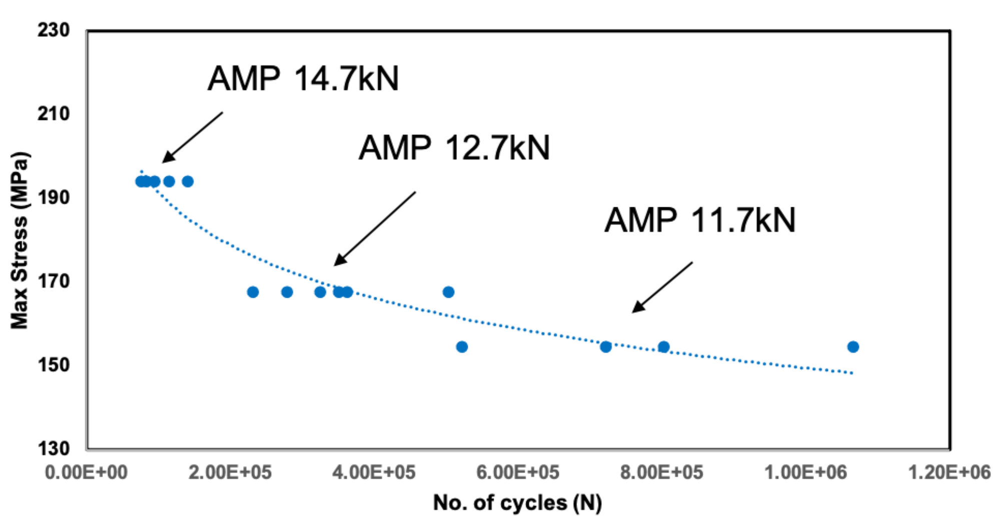

Figure 3.2: S-N curve for 5052-H32 aluminum alloy

3.2 Interrupted fatigue testing

The purpose of performing interrupted fatigue testing is to produce specimens at various fatigue levels by stopping the testing at several predetermined number of cycles. Considering the material cost and the time spent, the number of cycles applied to the specimens is set to be two levels, 33% and 67% fatigue life corresponding to the three loading amplitudes, 11.7, 12.7, and 14.7 kN. These specimens are used to represent the end-of-life products having different fatigue damage levels from the remanufacturing industry. Besides, three specimens without going through fatigue testing, i.e., 0% fatigue life, are included as specimens at the healthy state. The summary of

Table 3.1: Summary of the interrupted fatigue testing specimens

Specimen ID	Loading Amplitude (kN)	Percentage of Fatigue Life (%)	Max Stress Applied (MPa)
1	11.7	33	176
2	11.7	33	176
3	11.7	67	176
4	11.7	67	176
5	12.7	33	195
6	12.7	33	195
7	12.7	67	195
8	12.7	67	195
9	14.7	33	221
10	14.7	33	221
11	14.7	67	221
12	14.7	67	221
13	–	0	–
14	–	0	–
15	–	0	–

the interrupted fatigue testing specimens is presented in Table 3.1

3.3 Linear and nonlinear ultrasound measurements

In this research, linear ultrasonic (LU) and nonlinear ultrasonic (NLU) testing serve as the two main NDE methods for measuring the accumulated fatigue damage in the specimens. The ultrasonic testing is led by Prof. Matlack's group, and the testing system is shown in Figure 3.3. The LU and NLU measurements are both 1-D time domain signals, but the two approaches differ based on different theories and parameters, e.g., excitation wave shape, frequency, amplitude. Examples of LU and NLU signals are presented in Figure 3.4.

LU and NLU measurements were collected at nine locations in a specimen as illustrated in Figure 3.5, and each location was measured three times to understand the measurement repeatability. As a result, for each specimen, there are $9 \times 3 = 27$ signal profiles produced.

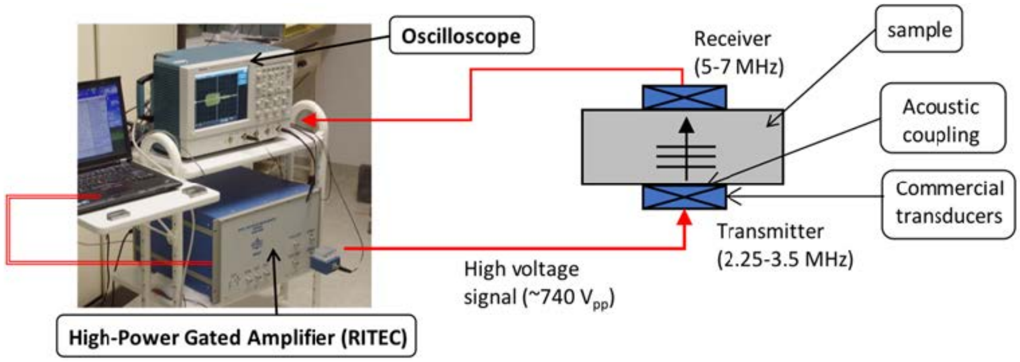

Figure 3.3: Experimental setup for LU and NLU at Prof. Matlack's Lab

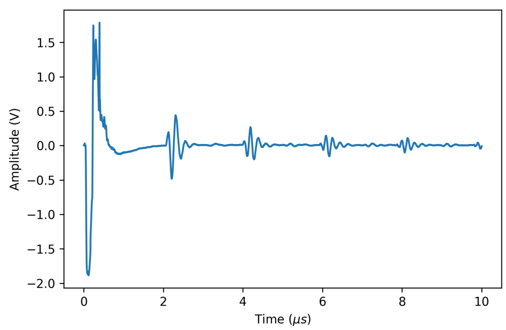

(a) Linear ultrasonic signal

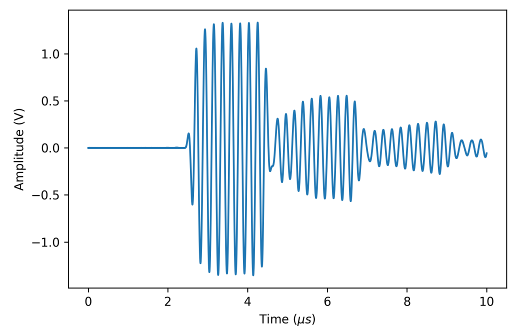

(b) Nonlinear ultrasonic signal

Figure 3.4: Examples of linear and nonlinear ultrasonic signals

3.4 X-ray diffraction measurement

Another quantity of interest, residual stress, is measured by X-ray diffraction (XRD) in this research. Residual stress is known to be associated with fatigue behaviors such as crack initiation and propagation. Besides, the full width at half maximum height (FWHM) of the diffraction peak in XRD is also extracted. Prof. Li's group performed the XRD measurements for a subset of specimens in the interrupted fatigue testing. The XRD data is used in the regression tasks in Chapter 6 as target variables.

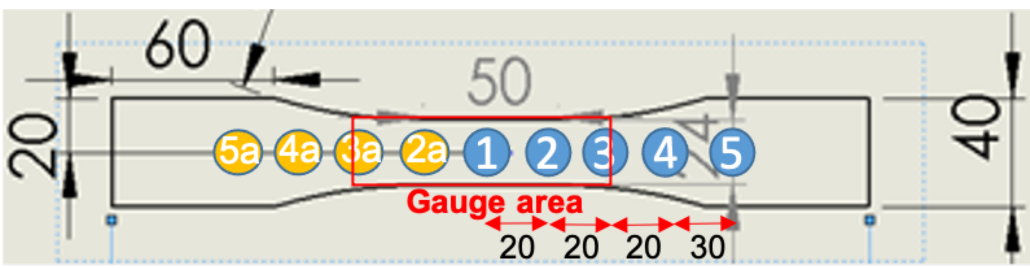

Figure 3.5: Schematic of the measurement locations for LU and NLU measurements. (The unit of length is in mm)

Chapter 4

Model Development

This chapter introduces a model development procedure used in both classification tasks in Chapter 5 and regression tasks in Chapter 6. The procedure involves: *a*) signal pre-processing, *b*) feature generation, *c*) feature selection, *d*) model training, *e*) model validation, and *f*) hyperparameter tuning, as shown in Figure .

4.1 Signal pre-processing

It is essential to reduce noises and extract regions of interest in signals by signal processing before we perform other analyses. Figure presents this process. First, DC bias was removed by subtracting the mean amplitude of a signal to prevent models from fitting on bias. Second, considering the computational cost from the high resolution data, we choose to downsample the ultrasonic signals. Third, we define the region or interest as the interval which contains the ultrasonic signal responses, and thus the other parts of a signal are discarded so that redundant information is not included.

4.2 Feature generation

Since ultrasonic sensor signals are unstructured, which is difficult to process, feature extraction methods are needed to create a representative set of values, i.e., features that aggregate the information from an entire signal. In this stage, physics-based and data-driven features are generated. The hybrid feature pool enables us to incorporate both physics knowledge and data-driven information into models.

4.2.1 Physics-based features

Given that physics modeling is built on theories or comprehensive experiment studies, physics-based features are robust, explainable, and suitable for applications having limited amounts of data such as the fatigue testing data in this research. Therefore, features from traditional LU and NLU testings become potential candidates for the model.

- Wave velocity

  In LU testing, ultrasonic wave velocity is a stiffness based measure which is associated with macroscopic damage such as crack/void coalescence and propagation. The wave speed is the distance divided by the time-of-flight (TOF) that a ultrasonic wave transverses in the material, as shown by Equation (4.1)

  $$v = \frac{2D}{\Delta t} \tag{4.1}$$

  where wave velocity is denoted by v, and D is the thickness of the specimen. Δt is the time difference between the actuation pulse and the response signal. Notice that, in our LU testing setup, one transducer severs as both the transmitter and receiver. Thus, the excitation signal travels $2D$ and the phase is changed $180°$ when received.

- Nonlinear acoustic parameter β

  While wave velocity from LU testing is able to detect fatigue damage at macro-scale, it is limited because it cannot detect defects much smaller than the probing wavelength, e.g., 1mm. In contrast, NLU techniques are based on a different physical principle: nonlinear elasticity from nano- and micro-scale defects induce harmonic generation. The nonlinear acoustic parameter is related to the amplitude of generated harmonics. This nonlinear parameter changes due to defects such as dislocations, local plastic strain, precipitates, and micro-cracks, all of which are orders of magnitude smaller than the probing wavelength. Here, we apply fast Fourier transform (FFT) to a NLU measurement and simply calculate the nonlinear parameter by using the ratio between the amplitudes of the fundamental and the harmonic waves given by Equation (4.2)

$$\beta = \frac{A_2}{A_1} \tag{4.2}$$

where A_1, A_2 is the amplitude of the fundamental wave and the second-order harmonic wave, respectively.

4.2.2 Data-driven features

The physics-based features alone, however, are not enough to capture all of the information from the LU and NLU signals. As a result, a large number of features engineered from the time domain, frequency domain, and time-frequency domain of ultrasonic measurements are added to the feature pool.

- Time domain features

  Time domain features are peak amplitudes, ratios between peak amplitudes, and components from Principal Component Analysis (PCA) and Independent Component Analysis (ICA). Statistics in time domain such as median, quantiles, variance, skewness, and kurtosis are also included. Besides, from the envelope analysis of a NLU signal, wave duration, wave energy, and the ratios between these quantities are calculated.

- Frequency domain features

  Frequency domain analysis offers some of the information that is not presented in the time domain. This information is especially valuable for periodic signals such as ultrasonic measurements. Thus, after applying fast Fourier transform (FFT), peak amplitudes, ratios between peak amplitudes, peak frequencies, frequency centroid and variance in FFT spectrum are extracted as the frequency domain features.

- Time-frequency domain features

  Ultrasonic signals are usually not stationary, i.e., frequency changes in time, because the interaction between ultrasonic waves and discontinuities within the material. Therefore, time-frequency analysis is needed to describe the phenomena. Discrete wavelet transform (DWT) is adopted to decompose ultrasonic measurements into several frequency bands. Then, statistics such as mean, median, kurtosis, and skewness are recorded for each frequency band.

We concatenate features from LU and NLU testing together, and thus the feature pool contains XXX features in total. A list of candidate features for LU and NLU measurements is displayed in Table

4.3 Feature selection

Feature selection aims to remove features that are redundant. Irrelevant features are common to see when we construct features without fully understanding a physical process. For example, the relationship between fatigue mechanism and ultrasonic responses. By including only the best subset of features for a prediction task, feature selection helps develop robust models against overfitting and improve model generalizability. There exists various feature selection techniques which can be mainly classified into three categories: filter methods, wrapper methods, and embedded methods. Each of these methods has its advantages, disadvantages, and suitable application scenarios.

In the model development pipeline, we adopted a wrapper method called Recursive Feature Elimination with Cross-validation (RFECV) to obtain the optimal feature subset that achieves the best predictive performance in multiple training/test data splits for a single model. Figure X shows the RFECV algorithm. First, recursive feature elimination (RFE) starts from a set with all available features and eliminate k features step by step based on the feature ranking with regressors/classifiers until the predetermined number of features n is reached. Nevertheless, the best number of features to select n^* is not determined. To find out n^* while alleviating the problem of overfitting, cross-validation (CV), a statistical model validation technique, is used along with RFE. CV partitions a dataset into training set and validation set in each fold. A model is evaluated multiple times with different partitions, and n^* is determined by the overall validation results. Then, RFE selects the optimal n^* features from the feature pool. We choose 5-fold classification in this feature selection procedure to avoid adding too much computation cost due to the fact that RFE is already computationally expensive.

4.4 Model training and validation

Model training and validation involve another CV loop. However, the CV here is not for finding the best feature subset but for providing a generalized estimate of a model's performance. Specifically, leave-one-group-out CV (LOGOCV) is applied, where each group contains three repeated measurements at one measurement location in one specimen. Here, we make an assumption that each group, i.e., each measurement location in a specimen, is an independent sample because of the differences in microstructure. In LOGOCV, each group is tested once and received validation scores by a predictor trained on the other groups, which efficiently utilizes the dataset and assesses the generalization capacity of a model.

4.5 Hyperparameter tuning

Searching an optimal set of hyperparameters is another crucial stage that significantly influences model performance in ML model development. We use grid search accompanied with the validation scores from the LOGOCV to tune hyperparameter in a simple and faster manner. Grid search exhaustively considers all candidates from predefined hyperparameter combinations. The number of hyperparameters and the range of each hyperparameter vary in different learning algorithms. The detailed settings will be discussed in Chapter 5 and 6.

Chapter 5

Remaining Useful Life Prediction

In this chapter, we propose a framework for predicting RUL of EoL products based on the ultrasonic testing. The framework has two parts: *a*) a ML classification task and *b*) a RUL inference procedure based on a S-N curve. First, ultrasonic signals are fed into ML classifiers to predict the loading condition and the number of fatigue cycles that a sample has gone through. Second, we estimate RUL from a S-N curve with the predicted loading condition and fatigue cycles.

5.1 Problem formulation

Given the goal of predicting the RUL of EoL products, we need to formulate this as a ML problem first. In this section, We discuss possible formulations by considering the characteristics of the fatigue dataset and the impact on the ML system in practice.

5.1.1 Dataset

In this RUL prediction task, the dataset is constructed on the ultrasonic measurements on the interrupted fatigue testing specimens in Table 3.1. There are 15 specimens and each of these were measured at 9 locations alongside 3 repeated measurements, producing 405 observations in total. Notice that we treat one measurement location in one specimen as a sample in the model training and validation procedure with LOGOCV, as described in Section 4.4. Besides, each specimen is tested by a combination from 4 loading amplitudes and 3 fatigue levels (the percentage of fatigue life), which forms the labels of a specimen.

Table 5.1: Summary of the RUL prediction dataset

Specimen ID	Number of Measurement Locations	Number of Repeated Measurements	Label (amplitude, percent of fatigue life)
1 2	9	3	Class 1 (11.7 kN, 33%)
3 4			Class 2 (11.7 kN, 67%)
5 6			Class 3 (12.7 kN, 33%)
7 8			Class 4 (12.7 kN, 67%)
9 10			Class 5 (14.7 kN, 33%)
11 12			Class 6 (14.7 kN, 67%)
13 14 15			Class 0 (0 kN, 0%)

5.1.2 Target variables

Obviously, RUL is directly translated by the percentage of fatigue life that a sample has gone through. The percentage of fatigue life as a continuous target variable is normally treated as a regression task. However, since we only have 3 different percentage of fatigue life in the dataset, which is not ideal for regression modeling, we decided to view the percentage of fatigue life as a discrete variable and the problem becomes a classification task.

Loading amplitude is another target variable to be considered because loading condition affects the mechanism of fatigue damage in a material. For instance, at 33% fatigue life, a sample undergoes 11.7 kN loading and a sample undergoes 14.7 kN loading could exist different fatigue damages. Hence, we place a label that is a combination of loading amplitude and the percentage of fatigue life on each sample. Table 5.1 presents the labeled RUL prediction dataset.

5.2 Design of classifiers

In this section, classifiers are designed for predicting the loading condition (amplitude) and the percent of fatigue life that a sample had experienced. Several classifiers are developed and the performance of each of those methods is evaluated based on the model development procedure in Chapter 4.

5.2.1 Multi-class classifier

A multi-class classifier is trained to classify a sample into one of the 7 classes. Figure XXX shows the inference process of a multi-class classifier. In multi-class problems, the classes are mutually exclusive. For example, class 1 and class 3 have nothing related. Despite we claimed that various loading conditions result in different fatigue behaviors in material, however, some similarities are still existed, e.g., at 33% fatigue life, samples undergone 11.7 kN and 12.7 kN are expected to be on a similar damage level. This idea can be applied to the commonality in samples at different percents of fatigue life as well. With the assumption about mutual exclusivity, multi-class formulation does not capture these characteristics of the data.

5.2.2 Multi-output classifier

On the other hand, multi-output classification is capable of dealing with mutually non-exclusive classes by predicting the loading amplitude and percentage of fatigue life separately. A multi-output classier outputs multiple labels, where each label is considered a multi-class classification problem. In this design, we build one classifier for predicting the loading amplitude from input signals; another one for classifying a signal into one of the percentages of fatigue life. Then, the two predicted labels are combined based on a rule-based algorithm to output a class label that is consistent with the label in the dataset, as depicted in Figure XXX. We call these two classifiers loading amplitude classifier (LAC) and fatigue cycle classifier (FCC), respectively. Each of the two classifiers are trained separately with the same model development procedure but different target variables. As a result, unlike the single multi-class classifier trying to learn a way to separate 7 classes, the multi-output classification builds LAC for a 4-class problem for loading amplitude and FCC for a 3-class problem for the percentage of fatigue life, which makes the problems easier to learn.

5.2.3 Two-stage classifier

Table XXX shows the design of a two-stage classifier. Extended from the idea of multi-output classifier in Subsection 5.2.2, a two-stage classifier is a classifier chains which predicts the loading amplitude and percentage of fatigue life in an order. The classification starts with a LAC and the predicted loading amplitude is added to the feature space of a $\text{FCC}_{\text{two-stage}}$. By utilizing the predicted label as a feature for next classifiers, the label dependence is preserved, i.e., the prediction of the percentage of fatigue life sample has undergone is associated with its loading amplitude. In this case, we put the LAC before the $\text{FCC}_{\text{two-stage}}$ because sometimes the loading condition is given in real life scenarios. Note that, in the training phase, the true loading amplitude is used to train the $\text{FCC}_{\text{two-stage}}$, but the $\text{FCC}_{\text{two-stage}}$ takes the predicted loading amplitude as one of the input features to do inference.

5.2.4 Hierarchical classifier

We further transform the multi-output task into a hierarchical classification scheme which is composed of multiple local classifiers based on a tree structure, shown in Figure XXX. One advantage of the hierarchical classification is to exploit parent-child class relationships present in the class hierarchy. Here, we train local classifiers per parent node in the taxonomy of the hierarchical classification problem. Specifically, one LAC and three FCCs for each loading amplitude are built, where each of the FCCs are trained by samples with the corresponding loading amplitude only. A prediction is inferred by the following manner: *a*) the LAC first output the loading amplitude for input LU and NLU signals. *b*) the predicted loading amplitude is also used to choose one of the FCCs for predicting the percentage of fatigue life. *c*) the FCC predicts the percentage of fatigue life. For example, 11.7 kN loading amplitude is predicted by the LAC. Therefore, $\text{FCC}_{11.7\text{ kN}}$ where the subscript stands for the loading amplitude that the classier corresponds to, is selected and outputs a 33% fatigue life prediction. Finally, the predicted result is Class 1 (11.7 kN, 33%).

5.2.5 Evaluation metrics

We calculate accuracy, recall, precision, and F1-measure to evaluate a classifier's performance with the LOGOCV result, and confusion matrices are also presented. Although there exist other evaluation metrics for multi-output problems, we evaluate the aforementioned classifiers in a unified multi-class classification problem with the label defined in Table 5.1. Thus, these classifiers are comparable with each other. Since there is not much class imbalance in the dataset, accuracy is an overall indicator for a model's performance. Furthermore, the model's performance on each class is provided by recall, precision and F1-measure. Finally, confusion matrices serve as a visualization for summarizing the detailed result of the testing of a classifier. We let practitioners to decide the importance of each metric as it depends on different scenarios. For example, recall may be more important than precision in classifying highly-fatigued samples due to the consideration of safety.

5.2.6 Results

This subsection summarizes the results of the developed classifier designs. Table 5.2 presents the learning algorithms and the number of features determined by the model development procedure in Section 4. Figure 5.1 depicts the performance of each classifier design by class. It is noticed that the proposed hierarchical classifier outperforms the other methods discussed in Section 5.2 for every class except Class 6. Therefore, the hierarchical classifier is chosen to demonstrate the RUL estimation algorithm in the following sections.

The recall, precision, and F1-score of the hierarchical classifier is reported in Table 5.3, and Figure 5.2 presents the detail of the LOGOCV classification result for 405 measurements in the dataset from the hierarchical classifier. It is observed that class 0 has 100% recall rate and only 2 measurements in class 5 are wrongly classified into class 0, implying that healthy samples are distinguishable from other damaged samples. Similarly, both of class 1 and class 2 have 96.3% recall rate and few measurements are wrongly predicted

Table 5.2: Summary of classification algorithms and model performance

Design of Classifiers	Algorithm	No. Selected Features	Macro Average F1-score
Multi-class	Logistic regression	35	0.75
Multi-output	Logistic regression	59 (LAC) 51 (FCC)	0.77
Two-stage	Logistic regression	59 (LAC) 51 ($FCC_{\text{two-stage}}$)	0.80
Hierarchical	Logistic regression	59 (LAC) 10 ($FCC_{11.7\text{ kN}}$) 40 ($FCC_{12.7\text{ kN}}$) 6 ($FCC_{14.7\text{ kN}}$)	0.83

as these two classes, showing that the classifier can identify the samples undergone low-amplitude fatigue testing very well. In addition, even though class 3-6 have more misclassified data points, those errors are mostly situated in the same loading amplitude as the true class are, indicating the LAC is able to estimate the loading amplitude that a sample has been applied. With the overall accuracy being 85.2%, the proposed hierarchical classier achieves a promising result for this application.

5.3 RUL estimation with a S-N curve

In the proposed framework, after obtaining the predicted loading amplitude and percentage of fatigue life, we estimate the RUL for a sample with the S-N curve of that material.

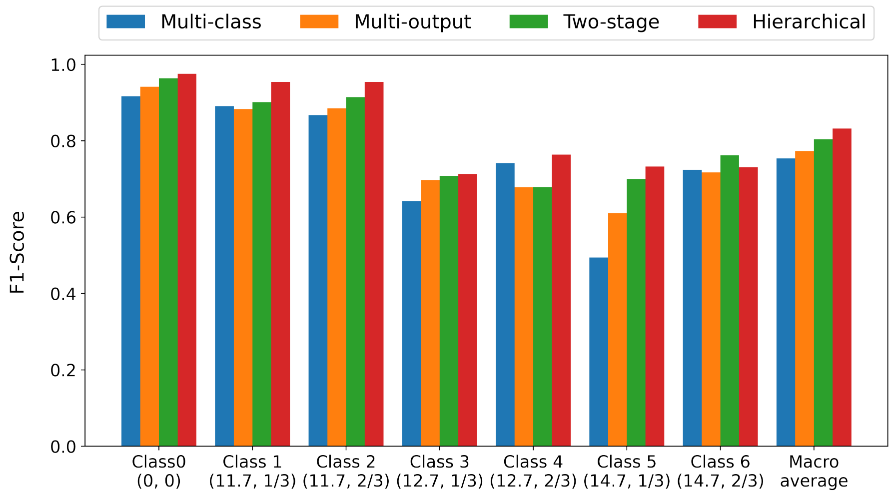

Figure 5.1: Comparison of F1-score by class and classifier designs

5.3.1 S-N curve with statistical distributions

Although a S-N curve is often referred to the best-fit line for fatigue data, fatigue life data can be modeled as statistical distributions to account for the variability in fatigue life. The randomness in the fatigue life comes from the stochastic behavior in fatigue process and the variance of microstructure in materials. As a result, the fatigue life has been widely modeled by statistical distributions including Gaussian (normal), log-normal, and Weibull distribution. Due to the limited amount of available fatigue life data in this research, we use a Gaussian normal distribution to model the fatigue life X_a at a loading amplitude a as

$$X_a \sim Normal(\bar{x_a}, \frac{s_a^2}{n_a}) \tag{5.1}$$

where $\bar{x_a}$ is the sample mean, s_a is the sample standard variance, and n_a is the sample size of fatigue data at loading amplitude a.

5.3.2 RUL inference procedure

A S-N curve serves as a look-up table for linking the classifier's predictions to the RUL. The inference procedure is detailed below:

1. Plotting the predicted loading amplitude and percentage of fatigue life. For example, the prediction, Class 1 (11.7 kN, 33% fatigue life), is

Table 5.3: Classification performance of hierarchical classifier

	Precision	Recall	F1-score	No. data
Class 0 (0 kN, 0%)	0.98	1.00	0.99	81
Class 1 (11.7 kN, 33%)	0.96	0.96	0.96	54
Class 2 (11.7 kN, 67%)	0.95	0.96	0.95	54
Class 3 (12.7 kN, 33%)	0.71	0.76	0.73	54
Class 4 (12.7 kN, 67%)	0.74	0.80	0.77	54
Class 5 (14.7 kN, 33%)	0.77	0.69	0.73	54
Class 6 (14.7 kN, 67%)	0.80	0.72	0.76	54
Macro Average	0.84	0.84	0.84	405
Weighted Average	0.85	0.85	0.85	405

plotted as the red dot in Figure XXX.

2. Determine the fatigue life with the corresponding loading amplitude from the S-N curve. The fatigue life can be in the format of a single value such as the median fatigue life or a statistical distribution.

3. If the fatigue life is represented by a value, the RUL can be estimated by Equation (5.2):

$$RUL = N_{fl} - N_c \tag{5.2}$$

where N_{fl} is the fatigue life from a S-N curve and N_c is the number of cycles translated from the predicted percentage of fatigue life a sample has undergone.

If the fatigue life at a given loading amplitude is modeled as a normal distribution, one way to estimate the RUL of a sample is to transform the fatigue life distribution by a factor of the predicted percentage of fatigue life, as in Equation (5.3) to (5.5):

$$X \sim Normal(\mu, \sigma^2) \tag{5.3}$$

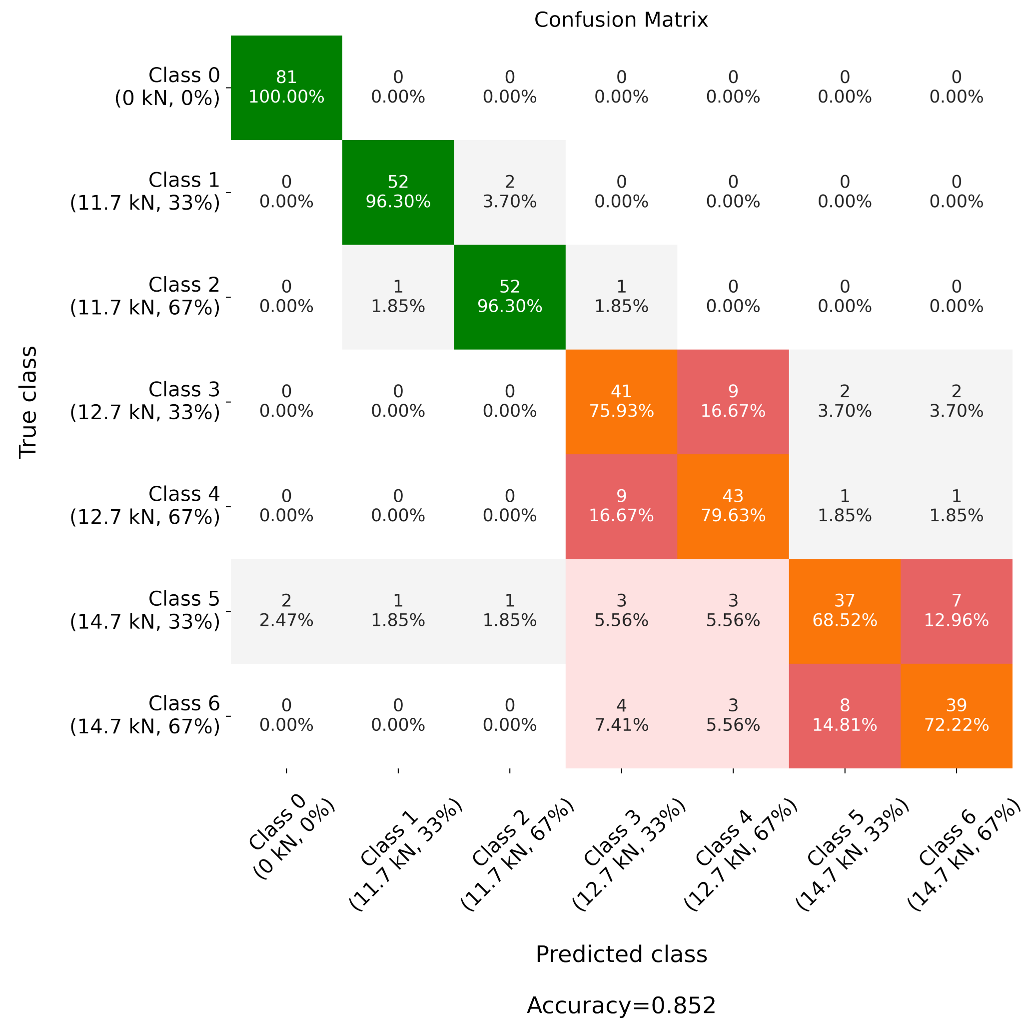

Figure 5.2: Confusion matrix of hierarchical classifier for cross-validation

$$Y = pX \tag{5.4}$$

$$Y \sim Normal(p\mu, p^2\sigma^2) \tag{5.5}$$

where Y is a random variable representing the RUL of a sample; X follows a normal distribution $Normal(\mu, \sigma^2)$ with μ as the mean and σ^2 as the variance of the fatigue life, and F is scaled by p which is the predicted percentage of fatigue life. Then, the point estimates, e.g., mean, median, or 25% quantile, as well as the interval estimate of RUL can be inferred. For instance, the 90% confidence interval of RUL is

$$CI = [\mu - z_{0.05}p\sigma,\ \mu + z_{0.95}p\sigma] \tag{5.6}$$

5.3.3 Examples

In this subsection, we demonstrate two examples of the RUL estimation based on the proposed framework. Because the true fatigue life of the testing samples in the interrupted fatigue testing data is not available, we cannot calculate the error of the RUL prediction for this stage. Instead, the estimated 90% confidence intervals of the RUL for specimen A and B are presented in Table X and X.

5.4 Discussion

One advantage of using the S-N curve to estimate RUL is that it can be quickly adopted to those materials whose S-N curve has constructed, which is common in the industry.

Table 5.4: RUL estimation for specimen 5

Specimen information
True label: Class 3 (12.7 kN, 33% fatigue life)
True number of cycles: 90011 cycles
Fatigue life from S-N curve: 342110 cycles
RUL calculated by true number of cycles: 252099 12.7 kN cycles

	Measurement Location								
Replicate	5a	4a	3a	2a	1	2	3	4	5
1	[114290, 341856] 12.7 kN (3)	[114290, 341856] 12.7 kN (3)	[114290, 341856] 12.7 kN (3)	[114290, 341856] 12.7 kN (3)	**[57145, 170928] 12.7kN (4)**	**[57145, 170928] 12.7kN (4)**	[114290, 341856] 12.7 kN (3)	[114290, 341856] 12.7 kN (3)	**[17340, 50523] 14.7kN (6)**
2	**[57145, 170928] 12.7kN (4)**	[114290, 341856] 12.7 kN (3)	[114290, 341856] 12.7 kN (3)	[114290, 341856] 12.7 kN (3)	**[57145, 170928] 12.7kN (4)**	**[57145, 170928] 12.7kN (4)**	**[17340, 50523] 14.7kN (6)**	[114290, 341856] 12.7 kN (3)	[114290, 341856] 12.7 kN (3)
3	[114290, 341856] 12.7 kN (3)	**[57145, 170928] 12.7kN (4)**	[114290, 341856] 12.7 kN (3)	[114290, 341856] 12.7 kN (3)	**[57145, 170928] 12.7kN (4)**	[114290, 341856] 12.7 kN (3)	[114290, 341856] 12.7 kN (3)	[114290, 341856] 12.7 kN (3)	[114290, 341856] 12.7 kN (3)

90% confidence interval in square brackets
Predicted class in parentheses
Bold text indicates misclassified measurements

Chapter 6

Residual Stress and FWHM Prediction

Because of the efficiency of ultrasonic testings in inspection area and cost, we explore the potential of using ultrasonic testings to measure quantities of interest which is originally obtained from XRD analysis. In this chapter, we present regression models for estimating the residual stress and the FWHM of XRD peaks on fatigue samples based on the ultrasonic measurements.

6.1 Problem formulation

Following the same manner in Section 5.1, we first translate the prediction tasks into ML regression problems based on the available dataset.

6.1.1 Dataset

The dataset for predicting residual stress and FWHM is composed of the XRD results and ultrasonic measurements. To obtain the residual stress and FWHM, the XRD analysis were performed on a subset of samples in the RUL dataset in Table 5.1, containing 8 specimens and 3 measurement locations for each specimen. Table 6.1 and 6.2 are the summary of the RS and FWHM dataset, respectively. It is worth mentioning that Specimen 7's relatively low FWHM values could indicate that there are microcrack initiations. Hence, we exclude samples from Specimen 7 in the FWHM prediction task.

6.1.2 Target variables

RS is known to influence the fatigue behaviors including crack initiation and propagation. FWHM is also an indicator for evaluating crack propagation.

Table 6.1: Summary of the RS prediction dataset

	Residual Stress (MPa)		
Specimen ID	Location 1	Location 2	Location 3
2	-61.7	-75.6	-80.2
4	-59.9	-69.6	-76.6
6	-60.3	-75.3	-79.6
7	-50.8	-59.6	-66.2
8	-57.3	-65.5	-79.7
10	-43.3	-47.0	-50.8
12	-38.8	-43.2	-50.0
14	-79	-76.7	-85.7

The negative sign indicates the compressive residual stresses.

Table 6.2: Summary of the FWHM prediction dataset

	FWHM (°)		
Specimen ID	Location 1	Location 2	Location 3
2	0.354	0.353	0.355
4	0.350	0.354	0.353
6	0.358	0.359	0.363
7	0.307	0.320	0.321
8	0.357	0.355	0.358
10	0.356	0.358	0.360
12	0.354	0.353	0.355
14	0.338	0.340	0.346

As a result, accurately predicting RS and FWHM based on ultrasonic measurements is beneficial to assist the fatigue level estimation and thus becomes the outcome of interest in this chapter. Here, the problem is formulated as two regression tasks: *a*) an univariate regression with RS as a target variable, and *b*) an univariate regression with FWHM as a target variable.

6.2 Residual stress prediction

In this section, the regression model for predicting RS based on ultrasonic signals is developed by following the procedure in Chapter 4. Mean absolute error (MAE), root mean squared error(RMSE), and mean absolute percentage error (MAPE) are used to asses the LOGOCV results. Table XXX compares the performance of ...

The best performing model for RS prediction is ... and Figure XXX displays the overall model performance by showing the actual and predicted RS, where a perfect model should follow the black line.

6.3 FWHM prediction

Similarly, the FWHM prediction model is built based on the procedure in Chapter 4 and is evaluated with the same metrics in Section 6.2. Table XXX is the comparison of model performance for candidate learning algorithms.

XXX achieves the best prediction result and its model performance is visualized in Figure XXX.

6.4 Discussion

Chapter 7

Conclusion and Future Work

7.1 Conclusion

A ML-based NDE methodology for assessing the accumulated fatigue damage level in terms of RUL, FWHM of XRD peak, and residual stress in recycled materials is developed, which aims to detect defects at various fatigue stages by combining the LU and NLU measurements and providing an ex-situ approach for the prognosis of useful life. An automatic pipeline is used to generate a pool of engineered features from raw ultrasonic signals, select useful features, validate models, and optimize classifiers and regressors appeared in this thesis.

A data-driven RUL prediction framework with the hierarchical classifiers and the statistical S-N curve is presented to bridge the research gap of RUL estimation in EoL products. The design of hierarchical classification scheme utilizes the characteristics of the fatigue dataset to predict the 7 combinations of the loading amplitude and the percent of fatigue life. Then, the use of statistical S-N curve incorporates the stochastic nature of fatigue life into the estimation of RUL. The framework relies on simple learning algorithms and does not require a large amount of data for training and validation, which shows the potential to be be quickly adopted to other materials.

In addition, two regression tasks for predicting residual stress and FWHM measured by XRD using ultrasonic testings both achieve high prediction accuracy. The little inconsistency between ultrasonic predictions and XRD measurements implies the potential to apply LU and NLU testings on measuring residual stress and other fatigue damage indicators in a more cost-efficient and faster way.

We envision the proposed NDE methodology and the prediction framework can will equip manufacturers with responsive screening of incoming recycled materials, and lead to a significant increase in using recycled materials for remanufacturing and high-quality products that meet customer expectations.

7.2 Future work

In practice, nevertheless, there exist several limitations for the current work and suggested future research efforts are discussed in the following directions.

7.2.1 Collect more data for model development and validation

More data is needed to make our models generalizable in real world applications even though we have utilized a cross-validation method, LOGOCV, to achieve good prediction accuracy while retaining the generalizability of the model performance with the limited amount of data. In the current LOGOCV, the group left out in the testing set is the 3 repeated measurements at one location; however, training data from neighboring locations at the same specimen still exist high similarity with the testing group, which causes the potential data leakage in the training phase. As a result, more data could enable better estimate of model performance by treating each specimen as a individual group in LOGOCV.

True fatigue life, i.e., the number of cycles which a sample fails at, for a interrupted fatigue testing specimen is required to justify the proposed RUL estimation framework. Currently, the samples used to generate the predicted RUL were not tested until fracture,which prevents us from quantifying the error of our RUL prediction. Besides, more fatigue life data allows us to fit the distributions more precisely and/or select a distribution family, e.g., Weibull, exponential, log-normal, etc., that better describes the fatigue life behavior. As a result, improvements in the accuracy and robustness of the RUL estimation can be achieved.

Additionally, a finer measurement interval can extend the classification task so that our classifiers can classify a sample into more fatigue levels, e.g., 15%, 33%, 50%, 67%, and 85%, or enable us to directly treat the estimation RUL as a regression task. With this, more advanced models can be researched and better applicability as well as flexibility for practitioners are expected.

7.2.2 Multi-sensor fusion for fatigue damage assessment

The integration of multiple sensors has the capability of detecting different types of defects and improving the robustness of fatigue damage evaluation. However, this work only studies the combination of LU and NLU testings. There are other NDE techniques such as infrared thermography, acoustic emission, etc., available to be added to the proposed NDE methodology. By integrating more sensors into the system, prediction performance will be further improved.

Moreover, sensor fusion can be categorized into several levels, e.g., data level, feature level, and decision level. We present a feature level fusion of LU and NLU signals in this thesis. Other fusion methods, especially decision level, are worth investigating because sensor selection can be conducted by for example, discarding sensors that degrade the model performance at different fatigue damage levels. Therefore, a cost-effective quantitative evaluation of fatigue progression system can be designed.

7.2.3 Spatial and temporal modeling for fatigue damage evaluation

With the measurements being made at multiple spatial locations and at multiple time increments, spatiotemporal modeling/interpolation can be performed and thus provide a full map containing the fatigue damage information for a specimen in space and time. For example, spatial statistics can be used to relate the correlation between measurement locations. Also, the temporal relation can also be modeled if enough data measured at different life time of a component. Having the spatiotemporal map for fatigue evolution can give practitioners a better understanding in the decision-making process.

References

[1] E. Santecchia, A. M. S. Hamouda, F. Musharavati, E. Zalnezhad, M. Cabibbo, M. El Mehtedi, and S. Spigarelli, "A review on fatigue life prediction methods for metals," *Advances in Materials Science and Engineering*, vol. 2016, p. 9573524, Sep 2016. [Online]. Available: https://doi.org/10.1155/2016/9573524

[2] B. Wisner, K. Mazur, and A. Kontsos, "The use of nondestructive evaluation methods in fatigue: A review," *Fatigue & Fracture of Engineering Materials & Structures*, vol. 43, no. 5, pp. 859–878, 2020. [Online]. Available: https://onlinelibrary.wiley.com/doi/abs/10.1111/ffe.13208

[3] J. Ben Ali, B. Chebel-Morello, L. Saidi, S. Malinowski, and F. Fnaiech, "Accurate bearing remaining useful life prediction based on weibull distribution and artificial neural network," *Mechanical Systems and Signal Processing*, vol. 56-57, pp. 150–172, 2015. [Online]. Available: https://www.sciencedirect.com/science/article/pii/S0888327014004087

[4] X. Li, Q. Ding, and J.-Q. Sun, "Remaining useful life estimation in prognostics using deep convolution neural networks," *Reliability Engineering & System Safety*, vol. 172, pp. 1–11, 2018. [Online]. Available: https://www.sciencedirect.com/science/article/pii/S0951832017307779

[5] J. Shi, T. Yu, K. Goebel, and D. Wu, "Remaining Useful Life Prediction of Bearings Using Ensemble Learning: The Impact of Diversity in Base Learners and Features," *Journal of Computing and Information Science in Engineering*, vol. 21, no. 2, 10 2020, 021004. [Online]. Available: https://doi.org/10.1115/1.4048215

[6] B. He, L. Liu, and D. Zhang, "Digital Twin-Driven Remaining Useful Life Prediction for Gear Performance Degradation: A Review," *Journal of Computing and Information Science in Engineering*, vol. 21, no. 3, 02 2021, 030801. [Online]. Available: https://doi.org/10.1115/1.4049537

[7] A. Mosallam, K. Medjaher, and N. Zerhouni, "Data-driven prognostic method based on bayesian approaches for direct remaining useful life prediction," *Journal of Intelligent Manufacturing*, vol. 27,

no. 5, pp. 1037–1048, Oct 2016. [Online]. Available: https://doi.org/10.1007/s10845-014-0933-4

[8] X. Li, Q. Ding, and J.-Q. Sun, "Remaining useful life estimation in prognostics using deep convolution neural networks," *Reliability Engineering & System Safety*, vol. 172, pp. 1–11, 2018. [Online]. Available: https://www.sciencedirect.com/science/article/pii/S0951832017307779

[9] J. Wu, K. Hu, Y. Cheng, H. Zhu, X. Shao, and Y. Wang, "Data-driven remaining useful life prediction via multiple sensor signals and deep long short-term memory neural network," *ISA Transactions*, vol. 97, pp. 241–250, 2020. [Online]. Available: https://www.sciencedirect.com/science/article/pii/S0019057819302939

[10] M. H. Lipu, M. Hannan, A. Hussain, M. Hoque, P. J. Ker, M. Saad, and A. Ayob, "A review of state of health and remaining useful life estimation methods for lithium-ion battery in electric vehicles: Challenges and recommendations," *Journal of Cleaner Production*, vol. 205, pp. 115–133, 2018. [Online]. Available: https://www.sciencedirect.com/science/article/pii/S0959652618327793

[11] K. Liu, Y. Shang, Q. Ouyang, and W. D. Widanage, "A data-driven approach with uncertainty quantification for predicting future capacities and remaining useful life of lithium-ion battery," *IEEE Transactions on Industrial Electronics*, vol. 68, no. 4, pp. 3170–3180, 2021.

[12] J. Achenbach, "Quantitative nondestructive evaluation," *International Journal of Solids and Structures*, vol. 37, no. 1, pp. 13–27, 2000. [Online]. Available: https://www.sciencedirect.com/science/article/pii/S0020768399000748

[13] J. Fan, X. Guo, and C. Wu, "A new application of the infrared thermography for fatigue evaluation and damage assessment," *International Journal of Fatigue*, vol. 44, pp. 1–7, 2012. [Online]. Available: https://www.sciencedirect.com/science/article/pii/S0142112312002046

[14] T. Kreis, "Application of digital holography for nondestructive testing and metrology: A review," *IEEE Transactions on Industrial Informatics*, vol. 12, no. 1, pp. 240–247, Feb 2016.

[15] A. J. K. M. Firdaus, R. Sloan, C. I. Duff, M. Wielgat, and J. F. Knowles, "Microwave nondestructive evaluation of thermal barrier coated turbine blades using correlation analysis," in *2016 46th European Microwave Conference (EuMC)*, 2016, pp. 520–523.

[16] J. W. Hennek, A. Nemiroski, A. B. Subramaniam, D. K. Bwambok, D. Yang, D. V. Harburg, S. Tricard, A. K. Ellerbee,

and G. M. Whitesides, "Using magnetic levitation for non-destructive quality control of plastic parts," *Advanced Materials*, vol. 27, no. 9, pp. 1587–1592, 2015. [Online]. Available: https://onlinelibrary.wiley.com/doi/abs/10.1002/adma.201405207

[17] N. R. Joshi and R. E. Green, "Ultrasonic detection of fatigue damage," *Engineering Fracture Mechanics*, vol. 4, no. 3, pp. 577–583, 1972. [Online]. Available: https://www.sciencedirect.com/science/article/pii/0013794472900677

[18] P. B. Nagy, "Fatigue damage assessment by nonlinear ultrasonic materials characterization," *Ultrasonics*, vol. 36, no. 1, pp. 375–381, 1998, ultrasonics International 1997. [Online]. Available: https://www.sciencedirect.com/science/article/pii/S0041624X97000401

[19] K. H. Matlack, J.-Y. Kim, L. J. Jacobs, and J. Qu, "Review of second harmonic generation measurement techniques for material state determination in metals," *Journal of Nondestructive Evaluation*, vol. 34, no. 1, p. 273, Nov 2014. [Online]. Available: https://doi.org/10.1007/s10921-014-0273-5

[20] J. H. Cantrell, "Ultrasonic harmonic generation from fatigue-induced dislocation substructures in planar slip metals and assessment of remaining fatigue life," *Journal of Applied Physics*, vol. 106, no. 9, p. 093516, 2009. [Online]. Available: https://doi.org/10.1063/1.3254223

[21] S. Sambath, P. Nagaraj, and N. Selvakumar, "Automatic defect classification in ultrasonic ndt using artificial intelligence," *Journal of Nondestructive Evaluation*, vol. 30, no. 1, pp. 20–28, Mar 2011. [Online]. Available: https://doi.org/10.1007/s10921-010-0086-0

[22] G. Tripathi, H. Anowarul, K. Agarwal, and D. K. Prasad, "Classification of micro-damage in piezoelectric ceramics using machine learning of ultrasound signals," *Sensors*, vol. 19, no. 19, 2019. [Online]. Available: https://www.mdpi.com/1424-8220/19/19/4216

[23] C.-S. Man and W. Y. Lu, "Towards an acoustoelastic theory for measurement of residual stress," *Journal of Elasticity*, vol. 17, no. 2, pp. 159–182, Jan 1987. [Online]. Available: https://doi.org/10.1007/BF00043022

[24] E. Tanala, G. Bourse, M. Fremiot, and J. De Belleval, "Determination of near surface residual stresses on welded joints using ultrasonic methods," *NDT & E International*, vol. 28, no. 2, pp. 83–88, 1995. [Online]. Available: https://www.sciencedirect.com/science/article/pii/096386959400013A

[25] H. Liu, Y. Li, T. Li, X. Zhang, Y. Liu, K. Liu, and Y. Wang, “Influence factors analysis and accuracy improvement for stress measurement using ultrasonic longitudinal critically refracted (lcr) wave,” *Applied Acoustics*, vol. 141, pp. 178–187, 2018. [Online]. Available: https://www.sciencedirect.com/science/article/pii/S0003682X18302056

[26] H. Baumgartl, J. Tomas, R. Buettner, and M. Merkel, “A deep learning-based model for defect detection in laser-powder bed fusion using in-situ thermographic monitoring,” *Progress in Additive Manufacturing*, vol. 5, no. 3, pp. 277–285, Sep 2020. [Online]. Available: https://doi.org/10.1007/s40964-019-00108-3

[27] C. Stadter, M. Schmoeller, L. von Rhein, and M. F. Zaeh, “Real-time prediction of quality characteristics in laser beam welding using optical coherence tomography and machine learning,” *Journal of Laser Applications*, vol. 32, no. 2, p. 022046, 2020. [Online]. Available: https://doi.org/10.2351/7.0000077

[28] T. Loutas, N. Eleftheroglou, and D. Zarouchas, “A data-driven probabilistic framework towards the in-situ prognostics of fatigue life of composites based on acoustic emission data,” *Composite Structures*, vol. 161, pp. 522–529, 2017. [Online]. Available: https://www.sciencedirect.com/science/article/pii/S0263822316316506

[29] A. Ray and S. Tangirala, “Stochastic modeling of fatigue crack dynamics for on-line failure prognostics,” *IEEE Transactions on Control Systems Technology*, vol. 4, no. 4, pp. 443–451, 1996.

[30] T. Peng, J. He, Y. Xiang, Y. Liu, A. Saxena, J. Celaya, and K. Goebel, “Probabilistic fatigue damage prognosis of lap joint using bayesian updating,” *Journal of Intelligent Material Systems and Structures*, vol. 26, no. 8, pp. 965–979, 2015. [Online]. Available: https://doi.org/10.1177/1045389X14538328

[31] P. Banerjee, R. P. Palanisamy, M. Haq, L. Udpa, and Y. Deng, “Data-driven prognosis of fatigue-induced delamination in composites using optical and acoustic nde methods,” in *2019 IEEE International Conference on Prognostics and Health Management (ICPHM)*, June 2019, pp. 1–10.

[32] X.-S. Si, W. Wang, C.-H. Hu, and D.-H. Zhou, “Remaining useful life estimation – a review on the statistical data driven approaches,” *European Journal of Operational Research*, vol. 213, no. 1, pp. 1–14, 2011. [Online]. Available: https://www.sciencedirect.com/science/article/pii/S0377221710007903

[33] Y. Lei, N. Li, L. Guo, N. Li, T. Yan, and J. Lin, "Machinery health prognostics: A systematic review from data acquisition to rul prediction," *Mechanical Systems and Signal Processing*, vol. 104, pp. 799–834, 2018. [Online]. Available: https://www.sciencedirect.com/science/article/pii/S0888327017305988

[34] S. Khan and T. Yairi, "A review on the application of deep learning in system health management," *Mechanical Systems and Signal Processing*, vol. 107, pp. 241–265, 2018. [Online]. Available: https://www.sciencedirect.com/science/article/pii/S0888327017306064

[35] H. J. Lim, H. Sohn, and Y. Kim, "Data-driven fatigue crack quantification and prognosis using nonlinear ultrasonic modulation," *Mechanical Systems and Signal Processing*, vol. 109, pp. 185–195, 2018. [Online]. Available: https://www.sciencedirect.com/science/article/pii/S088832701830116X

[36] M. Mazhar, S. Kara, and H. Kaebernick, "Remaining life estimation of used components in consumer products: Life cycle data analysis by weibull and artificial neural networks," *Journal of Operations Management*, vol. 25, no. 6, pp. 1184–1193, 2007, supply Chain Management in a Sustainable Environment Special Issue on Frontiers of Empirical Supply Chain Research. [Online]. Available: https://www.sciencedirect.com/science/article/pii/S0272696307000204

[37] G. Webster and A. Ezeilo, "Residual stress distributions and their influence on fatigue lifetimes," *International Journal of Fatigue*, vol. 23, pp. 375–383, 2001. [Online]. Available: https://www.sciencedirect.com/science/article/pii/S0142112301001335

[38] J. GUO, H. FU, B. PAN, and R. KANG, "Recent progress of residual stress measurement methods: A review," *Chinese Journal of Aeronautics*, vol. 34, no. 2, pp. 54–78, 2021. [Online]. Available: https://www.sciencedirect.com/science/article/pii/S1000936119304170